Atmos. Chem. Phys., 13, 5189–5203, 2013
www.atmos-chem-phys.net/13/5189/2013/
doi:10.5194/acp-13-5189-2013

Atmospheric Chemistry and Physics Open Access

High-resolution mapping of combustion processes and implications for CO_2 emissions

R. Wang[1], S. Tao[1], P. Ciais[2,3], H. Z. Shen[1], Y. Huang[1], H. Chen[1], G. F. Shen[1], B. Wang[1], W. Li[1], Y. Y. Zhang[1], Y. Lu[1], D. Zhu[1], Y. C. Chen[1], X. P. Liu[1], W. T. Wang[1], X. L. Wang[1], W. X. Liu[1], B. G. Li[1], and S. L. Piao[1,2]

[1]Laboratory for Earth Surface Processes, College of Urban and Environmental Sciences, Peking University, Beijing 100871, China
[2]Sino-French Institute for Earth System Science, Peking University, Beijing 100871, China
[3]Laboratoire des Sciences du Climat et de l'Environnement, CEA CNRS UVSQ, 91191 Gif sur Yvette, France

Correspondence to: S. Tao (taos@pku.edu.cn)

Received: 28 May 2012 – Published in Atmos. Chem. Phys. Discuss.: 21 August 2012
Revised: 18 March 2013 – Accepted: 3 April 2013 – Published: 23 May 2013

Abstract. High-resolution mapping of fuel combustion and CO_2 emission provides valuable information for modeling pollutant transport, developing mitigation policy, and for inverse modeling of CO_2 fluxes. Previous global emission maps included only few fuel types, and emissions were estimated on a grid by distributing national fuel data on an equal per capita basis, using population density maps. This process distorts the geographical distribution of emissions within countries. In this study, a sub-national disaggregation method (SDM) of fuel data is applied to establish a global $0.1^\circ \times 0.1^\circ$ geo-referenced inventory of fuel combustion (PKU-FUEL) and corresponding CO_2 emissions (PKU-CO_2) based upon 64 fuel sub-types for the year 2007. Uncertainties of the emission maps are evaluated using a Monte Carlo method. It is estimated that CO_2 emission from combustion sources including fossil fuel, biomass, and solid wastes in 2007 was 11.2 Pg C yr^{-1} (9.1 Pg C yr^{-1} and 13.3 Pg C yr^{-1} as 5th and 95th percentiles). Of this, emission from fossil fuel combustion is 7.83 Pg C yr^{-1}, which is very close to the estimate of the International Energy Agency (7.87 Pg C yr^{-1}). By replacing national data disaggregation with sub-national data in this study, the average 95th minus 5th percentile ranges of CO_2 emission for all grid points can be reduced from 417 to 68.2 Mg km^{-2} yr^{-1}. The spread is reduced because the uneven distribution of per capita fuel consumptions within countries is better taken into account by using sub-national fuel consumption data directly. Significant difference in per capita CO_2 emissions between urban and rural areas was found in developing countries (2.08 vs. 0.598 Mg C/(cap. × yr)), but not in developed countries (3.55 vs. 3.41 Mg C/(cap. × yr)). This implies that rapid urbanization of developing countries is very likely to drive up their emissions in the future.

1 Introduction

The combustion of carbon-containing fuels emits CO_2 and pollutants (BP, 2008; Solomon et al., 2007; Bond et al., 2004). Global emission inventories of CO_2 and air pollutants were developed years ago (Marland et al., 1985; Andres et al., 1996; Penner et al., 1993). In view of data compilation difficulties, only a few major fuel types could be considered (Rayner et al., 2010; Oda and Maksyutov, 2011). For example, it can be important for policy makers to know the quantities of CO_2 emitted only from diesel fuel used by industry and vehicles (Davis et al., 2010). Moreover, the emission factors (EFs; the ratio of pollutant emitted per unit of fuel burned) of pollutants can differ by orders of magnitude among fuels or facilities (Bond et al., 2004; Zhang et al., 2007). In addition to fossil fuels, information on biomass and solid waste fuels is also desirable since they are among important sources of many pollutants (Bond et al., 2004; Andreae and Merlet, 2001). Emission inventories in administrative units (countries, provinces) are usually geo-referenced into gridded maps using population density as a proxy for where emissions are located (Bond et al., 2004; Andres et al., 1996; JRC/PBL, 2009) This method can create a spatial

bias, because the per capita emission ratio F_{cap} is not uniform, especially within developing countries (Zhang et al., 2007). In this regard, sub-national fuel data are more reliable (Gurney et al., 2009). To reduce the bias caused by downscaling country emissions using population density, a series of efforts has been made. For example, Rayner et al. (2010) developed a data assimilation method based on the distribution of nightlights and population to produce a global emission field (called FFDAS) at 0.25° resolution, in which the distribution of emission was smoother than that of traditional population-based inventories (Rayner et al., 2010). Finally, there is also a need for high spatial (and temporal) emission maps of CO_2 and pollutants for atmospheric dispersion modeling, because errors in dispersion modeling decrease with increasing resolution (Bocquet, 2005; Tie et al., 2010). Moreover, upcoming atmospheric CO_2 measurements at 10 km or finer resolutions (GOSAT, OCO-2 satellites, and regional networks) require detailed CO_2 emission inventories for the interpretation of atmospheric gradients (Yokota et al., 2009; Lauvaux et al., 2009; Pillai et al., 2010). In addition, uncertainties of CO_2 emission inventories have rarely been quantified on a grid, leading to difficulties in evaluating them (Bocquet, 2005).

We present a sub-national disaggregation method (SDM) of fuel data to produce $0.1° \times 0.1°$ inventories of fuel consumptions and CO_2 emissions over the globe (PKU-FUEL and PKU-CO_2, Peking University Fuel and CO_2 Inventories). The product covers 64 sectors for the year 2007. Sub-national fuel consumption data of the major (carbon) fuel types were collected in 45 countries (7094 $0.5° \times 0.5°$ grids for 36 European countries (EUCS-36), 7942 counties for China, Mexico, and USA, 161 states/provinces for India, Brazil, Canada, Australia, Turkey, and South Africa). These sub-national administrative units are hereafter referred to as sub-nationally disaggregated units (SDUs). Fuel data for SDUs in the 45 countries where these data could be obtained, and national data in other countries were disaggregated to a $0.1° \times 0.1°$ grid using various proxies to generate the PKU-FUEL and PKU-CO_2 emission maps. To show the improvement gained by using SDU fuel data, a mock-up inventory (Nat-CO_2) is generated based on the national fuel data and disaggregation (like in previous global emission maps) and compared to PKU-CO_2. The PKU-CO_2 emission maps also compared against two previous inventories: VULCAN (over the US) and ODIAC (over the globe). Finally, the PKU-CO_2 inventory is used to calculate the difference in per capita CO_2 emission between urban and rural areas.

2 Data and methodology

2.1 Combustion sources

PKU-FUEL and PKU-CO_2 were constructed around 64 fuel sub-types in 5 categories and 6 sectors (Table 1). A total of 223 countries/territories are classified into developing/developed countries based on the World Bank's criteria for 2007. This is shown in Table S1 (World Bank, 2010). Russia was divided into two territories (European Russia and Asian Russia), because sub-national fuel consumption data were only available for European Russia. Due to differences in data sources and data processing methods, the 64 fuel sub-types were further classified into 8 groups in Table 2. These groups are (1) wildfires, (2) aviation/shipping, (3) power stations, (4) natural gas flaring, (5) agricultural solid wastes, (6) non-organized waste incineration, (7) dung cakes, and (8) others. Generally, fuels consumed in various sectors were compiled at global/national level and further allocated to $0.1° \times 0.1°$ grids using various proxies. The methodology and data sources used to compile fuel consumption for all these sources are presented in Sects. 2.2 and 2.3.

2.2 Compilation of fuel consumption data

For Group 1 (wildfires), global $0.5° \times 0.5°$ wildfire carbon emissions from GFED3 (van der Werf et al., 2010) were converted to fuel consumption based on the used EFs and disaggregated to $0.1° \times 0.1°$ using vegetation density generated in another dataset by Friedl et al. (2002) as a proxy. For Group 2 (aviation/shipping), global fuel consumptions of aviation (IEA, 2010a, b) and shipping (Equasis, 2008) were allocated to $0.1° \times 0.1°$ using CO emissions as a proxy. CO emission maps from aviation (JRC/PBL, 2011) and shipping (Wang et al., 2008; Eyers, 2005) were taken from the literature. For Group 3 (power stations), fuel consumptions by 26 239 major power stations from the CARMA v2.0 list (covering 77 % of the fuels used for power generation and 40 % of the global total fossil fuel emission) were allocated to individual grid points where power plants are reported (Wheeler and Ummel, 2008; Ummel, 2012). National fuel consumptions by other (non CARMA) power stations were calculated by subtracting these included in the CARMA v2.0 dataset from the national total for each type of fuel (IEA, 2010a, b) and disaggregated to $0.1° \times 0.1°$ using population density as a proxy (ORNL, 2008). For Group 4 (gas flaring), fuel consumptions by natural gas flaring were derived using a regression model (Elvidge et al., 2009) based on nightlight satellite measurements from the Defense Meteorological Satellite Program (NOAA, 2011). For Group 5 (agricultural solid wastes), the quantities of agricultural wastes burned in individual countries (provinces in China) were derived from crop production statistics (MAC, 2008; FAO, 2010), production-to-residue ratios (Bond et al., 2004; Streets et al., 2003; Cao et al., 2005; Zhang et al., 2009; Yevich and Logan, 2003), and percentage of field burned residues (Bond et al., 2004). For Group 6 (non-organized waste burning), quantities of non-organized wastes combusted were calculated from total quantities of wastes generated (UNSD, 2010) and incineration rates (Bond et al., 2004; Zhang et al., 2009). For Group 7 (dung cakes), dung cake consumption data in India were compiled (TERI, 2008) and extrapolated to 12 other South

Table 1. Classification of the 64 fuel sub-types included in the inventory. The fuels are classified into 5 fuel categories and 6 sectors. They are also divided into 8 groups (as marked by the superscripts) depending on data sources and data processing methods. Percentages of fuel consumption data collected from the literature are listed in parentheses, while consumptions of the remaining fuels were calculated using the regression models listed in Table S3.

Sector	Coal	Petroleum	Natural gas	Solid wastes	Biomass
Energy production	anthracite (100 %)[3] bituminous coal (97.3 %)[3] lignite (99.4 %)[3] coking coal (100 %)[3] peat (100 %)[3]	gas/diesel (98.7 %)[3] residue fuel oil (96.7 %)[3] natural gas liquids (99.9 %)[3]	dry natural gas (95.9 %)[3] natural gas flaring[4]	municipal waste (99.9 %)[3] industrial waste (99.3 %)[3]	solid biomass (85.3 %)[3] biogas (100 %)[3]
Industry	anthracite excluding aluminum production (98.1 %)[8] bituminous coal excluding coke and brick production (98.0 %)[8] lignite (99.4 %)[8] coking coal (100 %)[8] peat (100 %)[8] bituminous coal used in coke production (99.1 %)[8] bituminous coal used in brick production [8] anthracite used in aluminum production[8]	gas/diesel (99.4 %)[8] residue fuel oil (95.7 %)[8] crude oil used in petroleum refinery (96.6 %)[8] natural gas liquids (98.6 %)[8]	dry natural gas (88.5 %)[8]	municipal waste (99.7 %)[8] industrial waste (99.5 %)[8]	solid biomass (99.2 %)[8] biogas (100 %)[8]
Transportation		vehicles gasoline (98.0 %)[8] vehicles diesel (98.1 %)[8] aviation gasoline (99.6 %)[2] jet kerosene (99.5 %)[2] ocean tanker[2] ocean container[2] ocean bulk and combined carries[2] general cargo vessels[2] non-cargo vessels[2] auxiliary engines[2] military vessels[2]			liquid biofuels (100 %)[8]
Residential and commercial	anthracite (94.4 %)[8] bituminous coal (97.3 %)[8] lignite (100 %)[8] coking coal (100 %)[8] peat (100 %)[8]	kerosene (99.2 %)[8] liquid petroleum gas (94.9 %)[8] natural gas liquids (96.0 %)[8]	dry natural gas (96.0 %)[8]	non-organized waste incineration (86.2 %)[6]	firewood (90.1 %)[6] straw (98.8 %)[6] dung cake [7] biogas (100 %)[8]
Agriculture		gas/diesel (99.9 %)[8]		open burning of agriculture solid waste (98.5 %)[5]	
Natural					forest fire[1] deforestation fire[1] woodland fire[1] savanna fire[1] peat fire[1]

and Southeast Asian countries by assuming equal per capita consumption of that fuel. Then, consumptions data for all solid wastes were disaggregated to $0.1^\circ \times 0.1^\circ$ using a population proxy from a global $0.8 \times 0.8\,km^2$ dataset (ORNL, 2008).

2.3 Sub-national fuel data disaggregation (PKU-FUEL)

For Group 8 (other fuel types), national fuel consumptions of EUCS-36 (IEA, 2010a, b) were disaggregated to $0.5^\circ \times 0.5^\circ$ grids using CO emission proxies from the European Monitoring and Evaluation Programme by sector (Table S2) (CEIP, 2011). National fuel consumption of Mexico (IEA, 2010a)

Table 2. Schematic methods for converting raw data into $0.1^\circ \times 0.1^\circ$ gridded fuel consumption database. For the 8 groups using different disaggregation approaches, the numbers of fuel sub-types are shown in parentheses.

No.	Group	Coverage	Raw data	Resolution	Conversion and prediction	$0.1^\circ \times 0.1^\circ$ disaggregation
1	wildfire (5)	globe	CO emissions	$0.5^\circ \times 0.5^\circ$	converted to $0.5^\circ \times 0.5^\circ$ fuel consumptions using CO emission factors	biomass (grass/trees) proxy
2	aviation and shipping (9)	globe	fuel consumption	global	none	CO emission proxy
3	power stations (13)	globe	fuel consumptions of 26 239 major stations	locations	none	allocated directly to grids
		globe	fuel consumptions of other stations in 139 countries	national	predicted for the other 84 small countries/territories using region-specific models	national population proxy
4	natural gas flaring (1)	globe	nighttime lights for gas flaring	$0.1^\circ \times 0.1^\circ$	converted to $0.1^\circ \times 0.1^\circ$ fuel consumptions based on a regression model	allocated directly to grids
5	agricultural solid wastes (1)	China	crop productions	provincial	converted to provincial fuel consumptions based on crop-specified production-to-residue ratios and province-specific percentages of crop residues burned in the field	sub-national population proxy
		other countries	crop productions of 206 countries/territories	national	converted to national fuel consumptions based on crop-specified production-to-residue ratios and region-specific percentages of crop residues burned in the field (those for the remaining 17 small countries/territories were omitted)	national population proxy
6	non-organized waste incineration (1)	globe countries/territories	municipal waste of 102	national	converted to national fuel consumptions using 1 % and 5 % incineration rates for developed and developing countries, respectively, and predicted for the other 111 small countries/territories using region-specific models	national population proxy
7	dung cakes (1)	SEA13[a]	India consumption	national	predicted for other 12 countries assuming the same per capita consumption	national population proxy
8	other fuels (33)	EUCS-36[b]	(1) fuel consumptions except for aluminum, coke, and brick productions. National data for 132 countries and state/provincial data for USA, China and C-6 (2) coke, aluminum, and brick productions for 132, 83, and 113 countries[e]	national	converted to $0.5^\circ \times 0.5^\circ$ fuel consumptions using CO emission proxy	sub-national population/road proxy[f]
		Mexico		national	converted to county fuel consumptions using CO emission proxy	sub-national population/road proxy[f]
		USA		state	converted to county fuel consumptions using CO emission proxy	sub-national population/road proxy[f]
		China		provincial	predicted for 2373 counties using region-specific models	sub-national population/road proxy[f]
		C-6[c]		provincial/state	none	sub-national population/road proxy[f]
		C-178[d]		national	predicted for other 84 small countries/territories using region-specific models in Table S3 (aluminum and brick productions for 140 and 110 small countries/territories not included were omitted).	national population/road proxy[f]

[a] SEA13: 13 South and Southeast Asian countries including India, Bangladesh, Bhutan, Brunei, Cambodia, Laos, Maldives, Myanmar, Nepal, Pakistan, Sri Lanka, Timor-Leste, and Vietnam. [b] EUCS-36: 36 European countries including Albania, Andorra, Austria, Belarus, Belgium, Bosnia and Herzegovina, Bulgaria, Croatia, Czech Republic, Denmark, Estonia, Finland, France, Germany, Greece, Hungary, Iceland, Italy, Latvia, Lithuania, Macedonia, Moldova, Netherlands, Norway, Poland, Portugal, Romania, Russia, Serbia and Montenegro, Slovakia, Slovenia, Spain, Sweden, Switzerland, Ukraine, and United Kingdom. [c] C-6: 6 countries with state/province data collected, including India, Brazil, Canada, Australia, Turkey, and South Africa. [d] C-178: 178 countries other than EUCS-36, C-6, USA, China, or Mexico. [e] Consumptions of bituminous (coke and bricks productions) and anthracite (aluminum production) were converted from the production volumes (1.25, 1.06, and 3 ton coal/ton coke, bricks, and aluminum produced, respectively). [f] Population proxy was applied to disaggregate fuel consumptions (the 15197 SDUs for the 45 countries and remaining 178 countries) to $0.1^\circ \times 0.1^\circ$ grids (ORNL, 2008) except for on-road gasoline and diesel vehicles, for which $0.1^\circ \times 0.1^\circ$ CO emission from road transportation in EDGAR v4.2 (JRC/PBL, 2011) was used as a proxy.

and state fuel consumptions of USA (USEIA, 2008) were allocated to counties using CO emissions by county as a proxy within Mexico or USA states by sector (Table S2) (USEPA, 2006, 2011). County-level fuel consumptions in China were determined based on the provincial fuel consumption (NBS, 2008) and a set of provincial-data-based regression models (Zhang et al., 2007). State/province fuel consumptions in India, Brazil, Canada, Australia, Turkey, and South Africa were directly compiled from the literature (TERI, 2008; Statistics South Africa, 2009; Brazil Energy Ministry, 2010; TSI, 2010; Environment Canada, 2010; ABES, 2008). National fuel consumptions for countries without sub-national fuel data were taken from the International Energy Agency (IEA) (IEA, 2010a, b) and other energy statistics (USGS, 2010a; UNID, 2008). Finally, a population proxy was applied to disaggregate fuel consumption (15197 SDUs in 45 countries and 178 remaining countries where no SDU data were available) to $0.1^\circ \times 0.1^\circ$ grids (ORNL, 2008). On-road gasoline and diesel vehicles fuel data were disaggregated at $0.1^\circ \times 0.1^\circ$ resolution from CO emission of the road transportation sector in EDGAR v4.2 (JRC/PBL, 2011). The methods of disaggregation for the different fuels and regions are summarized in Table 2. For the countries with no fuel data available, a set of region-specific regression models were developed to predict their fuel consumptions based on data from other countries in the same region (Table S3). Rural population, total population, and/or gross domestic production were used as independent variables (World Bank, 2010) in those regressions. In processing the sub-national data for these sectors in Group 8 (others), the sub-national

fuel data compiled in our local database are listed in Table S2. The fuel sub-types in Group 8 with detailed sub-national consumption data available are marked with a # superscript. For fuel sub-types without detailed data, the shares of these sub-types in sub-nationally disaggregated units (SDUs) were assumed to be equal to the national shares.

2.4 Development of PKU-CO_2 emission maps

Based on PKU-FUEL data, CO_2 emissions (PKU-CO_2) were calculated using CO_2 emission factors (EF_C) and the combustion rates for the different fuel types. EF_C for all combustion processes were derived as the means of data collected from the literature. Specially, EF_C for oil consumed in petroleum refinery industry was from Nyboer et al. (2006), and EF_C for oil consumed by 7 ship types and 5 types of biomass burning were collected from Wang et al. (2008) and van der Werf et al. (2010). For the remaining fuel types, EF_C were collected from URS (2003), IPCC (1996), US Department of Energy (2000), API (2001), and USEPA (2008). Fixed combusted rates of 0.990, 0.980, 0.995, 0.980, 0.901, 0.887, 0.789, 0.919, and 0.901 were applied to petroleum, coal, natural gas, solid municipal and industrial waste fuel, biomass burned in the field, firewood burned in cook stoves, firewood burned in fireplaces, crop residue burned in cook stoves, and open burning of agriculture waste, respectively (Johnson et al., 2008; Lee et al., 2005; Oda and Maksyutov, 2011; Zhang, et al., 2008). Although our study focuses on fuel and CO_2 emissions from fuel burning, CO_2 emissions from cement production were also compiled. These are based on cement production data in 155 countries (USGS, 2010b) and CO_2 emission factors from the literature (Andres et al., 1996). Country-level reported CO_2 emissions from cement production were disaggregated to $0.1^\circ \times 0.1.^\circ$ grids using industrial coal consumption maps from PKU-FUEL as a proxy, hence making the assumption that cement manufactures are co-located with coal consumption.

2.5 Accuracy of the location of the power plants

Fuel consumptions of 26 239 major power plants from the CARMAv2.0 contribute 77 % of the fuels used for power generation (Wheeler and Ummel, 2008; Ummel, 2012). Being the important point sources of CO_2 emission, the positions of these power plants were tested before being used in PKU-FUEL and PKU-CO_2. The locations for 350 randomly selected power plants were checked one by one in Google imagery for all countries except the USA where the geolocations have been proved to be accurate (Wheeler and Ummel, 2008). The results are shown in Fig. S1. It was found that 45 % (China) and 89 % (countries other than China and the USA) of the stations are located in the same grid points ($0.1^\circ \times 0.1^\circ$) as reported in the CARMA v2.0 database, and that the remaining 42 % (China) and 9 % (countries other than China and USA) of stations are actually located in grids adjacent to the one listed in CARMA v2.0. This suggests that the accuracy of the CARMA v2.0 power plant locations is satisfactory for $0.1^\circ \times 0.1^\circ$ resolution mapping, except for China. Spatial localization errors in China are relatively large. Yet, for 87 and 95 % of Chinese power stations, the differences between the CARMA v2.0 reported locations and actual locations found by Google imagery are no more than 2 (20 km) and 3 (30 km) grids, respectively. Although CARMA v2.0 was the best global power station dataset available for the year of 2007, the location of power plants is expected to be updated when the new CARMA version product is published or a new dataset is available.

2.6 Fuel and CO_2 emission-map uncertainties from Monte Carlo simulations

Monte Carlo ensemble simulations of the PKU-FUEL and PKU-CO_2 emission models were calculated 1000 times on all grids. We randomly varied input data given an a priori uncertainty distributions with a coefficient of variation (CV). CVs of fuel consumptions from ships/aviation and wildfires are set to be 20 and 18 %, respectively, with normal distributions (Wang et al., 2008; van der Werf et al., 2010). A CV of 10 % was adopted for all other fuel data, with a uniform distribution (Ciais et al., 2010; Marland et al., 2008). To consider the uncertainty associated with spatial disaggregation of fuel data, a CV was defined for each SDU (subnationally disaggregated unit) or country (where no subnational data exist) according to their size. The formula is $CV_i = 1000\,\% \times N_i/225\,829$, where N_i is the number of grid points in a certain SDU/country, and 225 829 is the number of grid points in Asian Russia, the largest SDU of the world. A CV of 1000 % was assigned to this latter region. The CVs of literature-reported EF_C range from 3.8 % to 5.1 %. Thus, a constant value of 5 % was adopted with a normal distribution. The CVs of combustion rates were set to be 20 % with a normal distribution. The results of the Monte Carlo simulations are presented using the two metrics R_{90} (95th minus 5th percentile range) and R_{90}/M (R_{90}/median) that provide absolute and relative errors on a map, respectively.

2.7 Urban–rural per capita emissions contrast

For each country, a population density threshold value was defined to separate between urban and rural grid points, based on urbanization degree data (World Bank, 2010) and the spatial distribution of population density in 2007 (ORNL, 2008). The sensitivity of the result to the threshold value was tested by re-calculating E_{cap} of urban and rural grid points, with this threshold value multiplied by a factor varied from 0.8 to 1.2 at a 0.1 interval. It was found that, with a ± 10 % change in the threshold, the calculated E_{cap} changes only by 0.3–0.5 % (0.4–1.2 %) in rural areas and by 5.5–5.8 % (0.6–0.8 %) in urban areas for developing (developed) countries. This sensitivity test suggests that our classification method is

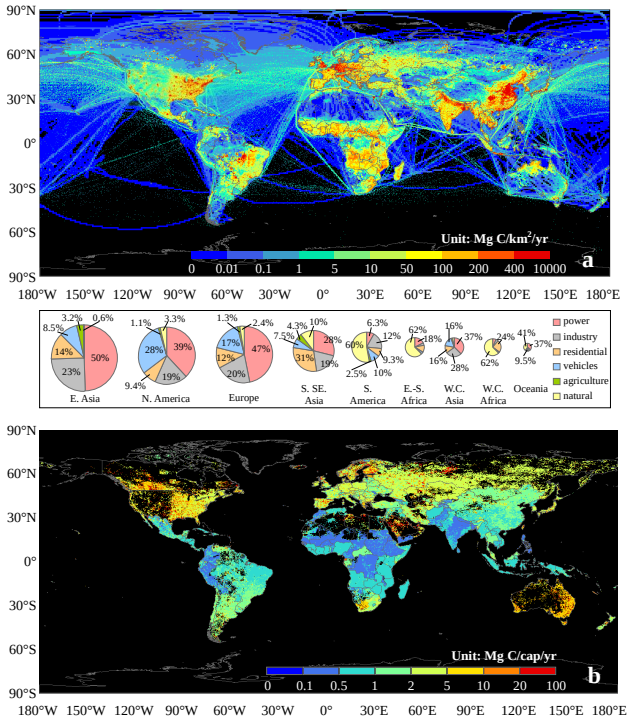

Fig. 1. Geographic distributions of total and per capita CO_2 emissions from combustion sources at $0.1° \times 0.1°$ resolution in 2007 from the PKU-CO_2 inventory developed in this study. **(a)** Total CO_2 emissions from all combustion sources and **(b)** per capita energy-related CO_2 emissions excluding shipping and aviation. For total emission of each region, the relative contribution of each sector is shown in the pie charts in the inset and the total area of each pie is proportional to the emission.

robust (Fig. S2). A CV in the threshold of 10 % (uniform distribution) was included in the Monte Carlo uncertainty characterization of urban and rural E_{cap} calculation.

2.8 Carbon balance of terrestrial ecosystem

For inverse modeling, the spatial distribution of terrestrial ecosystem CO_2 fluxes, $B(x)$ where x denotes the spatial coordinate, can be calculated by subtracting fossil fuel CO_2 emissions, $F(x)$, from the net land–atmosphere CO_2 flux distribution, $N(x)$. The result of the CarbonTracker inversion was used as $N(x)$ for the year 2007 (Peters et al., 2007). Two maps $B(x)$ were calculated as $B(x) = N(x) - F(x)$, with $F(x)$ being the emission maps either from PKU-CO_2 or from NAT-CO_2 (regridded to $1° \times 1°$ to match the resolution of $N(x)$ from CarbonTracker). The difference between the two maps of $B(x)$ obtained with the two $F(x)$ maps was calculated to illustrate the effect of using the sub-national (this study) instead of national fuel data (all atmospheric inversion studies) on terrestrial carbon fluxes.

3 Results

3.1 Global fuel consumption and CO_2 emission map in 2007

According to PKU-FUEL, oil ($154\,EJ\,yr^{-1}$), coal ($133\,EJ\,yr^{-1}$), and natural gas ($124\,EJ\,yr^{-1}$) dominated global fuel consumptions, followed by biomass ($11.4\,EJ\,yr^{-1}$) and solid waste ($3.59\,EJ\,yr^{-1}$) fuels. Globally, F_{cap} was $0.0733\,TJ/(cap. \times yr)$, which was primarily fossil fuel ($0.0650\,TJ/(cap. \times yr)$), while energy-related biomass ($0.00829\,TJ/(cap. \times yr)$) and solid waste fuels ($0.000611\,TJ/(cap. \times yr)$) contributed relatively small fractions. The mean F_{cap} for fossil fuels in developed countries ($0.172\,TJ/(cap. \times yr)$) was approximately 4 times of that of developing countries ($0.0414\,TJ/(cap. \times yr)$).

PKU-CO_2 was developed based on PKU-FUEL using EF_C, and combustion rates of various fuel types. Global CO_2 emission from all combustion sources was $11.2\,Pg\ C\,yr^{-1}$ in 2007. The largest contribution was from energy production (33.8 %), followed by industry (18.0 %), transportation (15.2 %), residential/commercial (14.8 %), and agriculture (2.1 %). Wildfires contributed 16.1 % of the total. Fossil, biomass, and solid waste fuels emitted 7.83, 3.18, and $0.224\,Pg\,C\,yr^{-1}$, respectively. The estimated fossil fuel emission of CO_2 ($7.83\,Pg\,C\,yr^{-1}$) is similar to the $7.87\,Pg\,C\,yr^{-1}$ reported by IEA (IEA, 2010c) but lower than the $9.06\,Pg\,C\,yr^{-1}$ from EIA (USEIA, 2010), in which non-fuel-use oil products were included.

For energy-related (excluding wildfires) fuel combustions, the global E_{cap} was $1.51\,Mg\ C/(cap. \times yr)$, with large variations among and within countries. For example, E_{cap} were 0.661 for India, compared to $5.74\,Mg\ C/(cap. \times yr)$ for USA. Moreover, among the 2373 counties in China, E_{cap} varied dramatically from 0.05 to $41.1\,Mg\ C/(cap. \times yr)$, confirming the value of sub-national data down to county level. Emissions from individual fuel sub-types are listed in Table 3. Figure 1 shows the geographical distributions of CO_2 emissions and E_{cap}, the relative contributions of the 6 sectors in 9 regions given in the pie charts. Emissions from aviation ($91\,Tg\,C\,yr^{-1}$) and shipping ($181\,Tg\,C\,yr^{-1}$) are not included in the pie charts. Regionally, power generation was the most important sector in North America (38.6 %), Western Europe (46.7 %), and East Asia (50.0 %), while savanna burning dominated in Africa (62.5 %), South America (59.6 %), and Oceania (40.9 %). Emissions from motor vehicles were the second largest contributor in North America (28.3 %) and Western Europe (16.7 %). In Fig. 1b, E_{cap} was high in the western USA because of relatively high fuel consumptions for transportation in states with low population densities: Wyoming, North Dakota and Texas (USEIA, 2008). For Alaska and northern Europe, more fuel was consumed for heating in winter. CO_2 emission maps separated by the major fuel categories and sectors are shown in Fig. S3. Information on both sectoral and regional CO_2 emissions is presented in

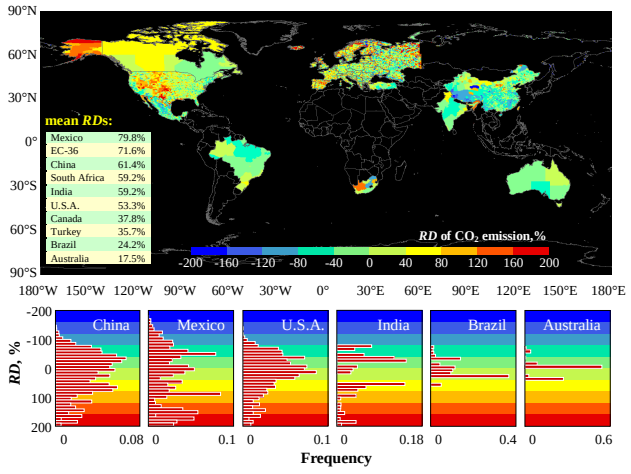

Fig. 2. Comparison of CO_2 emissions at the scale of sub-nationally disaggregated units (SDUs, e.g., counties, states/provinces, or 0.5° grids) in 45 countries between the sub-nationally (PKU-CO_2) and nationally (NAT-CO_2) disaggregated inventories. Relative differences (RDs) between the PKU-CO_2 and NAT-CO_2 inventory are calculated for all SDUs with sub-national fuel consumption data specially compiled for PKU-CO_2 ($0.5° \times 0.5°$ grids in EUCS-36, counties in China, Mexico, and USA, and states/provinces in India, Brazil, Canada, Australia, Turkey, and South Africa). Mean absolute RDs for these countries are listed at the bottom-left of the map. A positive value indicates an underestimation by national data disaggregation. Frequency distributions of RDs for China, Mexico, USA, India, Brazil, and Australia are shown in the bar charts at the bottom. The RD cannot be calculated for the countries where sub-national data are not available or not reported, and these areas are marked in black.

Table S4, which is valuable for emission prediction and regional mitigation policy formation.

3.2 Comparing PKU-CO_2 with emission maps obtained from national fuel data (NAT-CO_2)

To quantify the improvement expected in PKU-CO_2, a mock-up emission map (NAT-CO_2), excluding point (power stations/natural gas flaring), wildfires, and non-country-specific sources (aviation/shipping), was established using exactly the same method except that nationally aggregated fuel data and proxies were applied for the 45 countries where PKU-CO_2 uses sub-national data. Emissions calculated in the SDUs of the 45 countries were compared between PKU-CO_2 and NAT-CO_2 by calculating a relative difference $\mathrm{RD} = (E_1 - E_2)/((E_1 + E_2)/2)$ where E_1 and E_2 are mean emissions in each SDU from PKU-CO_2 and from the less accurate NAT-CO_2, respectively. E_1 is referred to as the more accurate value (MAV), since it is derived from actual fuel data in each SDU without minimum proxy and disaggregation error. By comparison, E_2 is associated with geographic bias induced by the disaggregation to smaller scales. In other words, RD is a metric of how bias of regional CO_2 emissions can be reduced by using sub-national fuel data. The larger the RD value, the more realistic PKU-CO_2 is over NAT-CO_2.

The 45 countries with sub-national fuel data available represented 45, 61, and 69 % of the global total area, population, and fuel consumption, respectively. Within these countries, CO_2 emissions were computed from the actual fuel data of 15 197 SDUs instead of from the national fuel data like former studies (Andres et al., 1996; Oda and Maksyutov, 2011). Although residual errors still occurred when disaggregating the emissions from SDUs to the $0.1° \times 0.1°$ grids in PKU-CO_2, these errors should be much smaller than the errors induced by disaggregating the emissions from a country's total to $0.1° \times 0.1°$ grids of NAT-CO_2. In fact, the average area of all SDUs is only 4560 km^2, compared to 1 330 108 km^2 of the 45 countries, leading to a significant reduced spatial bias in the CO_2 emission distribution. Figure 2 shows the spatial distribution of RD for the 15 197 SDUs between PKU-CO_2 and the less accurate NAT-CO_2 emission maps. In the 9 countries with county or state/provincial data used in PKU-CO_2, the country averages of RD values in all SDUs range from 17.5 % (Australia) to 79.8 % (Mexico). These large RD values indicate that a substantial reduction of the spatial bias of CO_2 emission can be achieved using the sub-national data. It was also found that the degree of the spatial bias reduction is larger in countries with higher F_{cap} heterogeneity (e.g., large developing countries) or with smaller SDUs (e.g., countries with county fuel data).

3.3 Uncertainty of PKU-CO_2

Monte Carlo simulations were applied to estimate uncertainties on CO_2 emission maps associated with uncertain fuel data and uncertain activity data in the spatial disaggregation process. The result is that R_{90} for global total CO_2 emission in 2007 was 4.19 (range 9.11–13.3) Pg C yr^{-1} (see Table 3 for R_{90} of the 64 individual fuel types). For the spatial distribution of CO_2 emissions, the absolute and relative uncertainties (R_{90} and R_{90}/M) are shown as maps in Fig. 3. Mean R_{90} and R_{90}/M of gridded emissions for the 45 countries with sub-national data were 62.4 Mg km^{-2} yr^{-1} and 63.2 % for PKU-CO_2, compared to 417 Mg km^{-2} yr^{-1} and 364 % for NAT-CO_2. This shows that a substantial reduction in the uncertainty of CO_2 emission maps can be reached with the patient effort of collecting sub-national data. In Fig. 3, the highest R_{90} values can be found in large countries where sub-national fuel data are not available, such as Indonesia and Pakistan, and in areas with very high emission densities such as northern China and Western Europe.

3.4 Comparison of PKU-CO_2 with ODIAC and VULCAN 2.2 inventories

The PKU-CO_2 emission map is compared with the ODIAC one (global fossil fuel, 2007, satellite nightlight-based, 1 km × 1 km, converted to $0.1° \times 0.1°$ for the comparison)

Table 3. Energy and CO_2 emissions from 64 fuel sub-types and cement production in 2007. Medians and R_{90} (95th minus 5th percentile range) were used for estimating the emissions and characterizing the uncertainties. CO_2 emission fractions (F) are listed for individual fuel sub-types. The emission from cement production is included in the last two rows so as to provide a complete emission inventory of CO_2.

Sector	Type	Detailed sub-type	Energy, EJ yr^{-1}	CO_2, Tg C yr^{-1}	F, %	R_{90}, Tg C yr^{-1}
Energy production	Coal	Anthracite used	0.875	22.37	0.19	18.87–25.86
		Coke used	0.765	21.00	0.18	17.72–24.29
		Bituminous coal used	90.142	2147.28	18.47	1811.35–2482.87
		Lignite used	20.313	512.43	4.41	432.28–592.53
		Peat used	0.342	9.21	0.08	7.77–10.65
	Petroleum	Gas/diesel used	2.806	49.75	0.43	41.98–57.50
		Residue fuel oil used	7.696	136.78	1.18	115.40–158.08
		Natural gas liquids used	0.001	0.01	0.00	0.01–0.02
	Gas	Dry natural gas used	48.821	662.63	5.70	559.04–765.87
		Natural gas flaring	5.348	73.56	0.63	62.05–85.02
	Biomass	Solid biomass used	6.487	150.98	1.30	127.37–174.58
		Biogas used	0.099	5.57	0.05	4.70–6.44
	Wastes	Municipal waste used	0.951	21.02	0.18	17.73–24.30
		Industrial waste used	0.222	4.76	0.04	4.02–5.51
	Sub-total		184.704	3800.02	32.68	3205.69–4393.50
Industry	Coal	Bituminous coal used in coke production	2.345	84.82	0.73	71.59–98.05
		Bituminous coal used in brick production	8.895	216.89	1.87	182.96–250.79
		Anthracite used in aluminum production	0.547	18.49	0.16	15.60–21.37
		Anthracite used	1.098	28.42	0.24	23.97–32.86
		Coke used	0.668	18.57	0.16	15.67–21.47
		Bituminous coal used	15.581	374.74	3.22	316.11–433.30
		Lignite used	0.659	16.73	0.14	14.11–19.35
		Peat used	0.031	0.82	0.01	0.70–0.95
	Petroleum	Gas/diesel used	5.847	111.45	0.96	94.03–128.80
		Residue fuel oil used	5.108	102.65	0.88	86.61–118.63
		Crude oil consumed in petroleum refinery	15.683	216.33	1.86	182.52–249.99
		Natural gas liquids used	0.059	0.97	0.01	0.82–1.12
	Gas	Dry natural gas used	46.100	639.56	5.50	539.58–739.27
	Biomass	Solid biomass used	6.487	180.80	1.55	152.53–209.07
		Biogas used	0.099	1.61	0.01	1.36–1.86
	Wastes	Municipal waste used	0.015	0.33	0.00	0.28–0.38
		Industrial waste used	0.226	5.09	0.04	4.29–5.89
	Sub-total		114.379	2018.27	17.36	1702.72–2333.17
Residential/ Commercial	Coal	Anthracite	0.074	2.56	0.02	2.15–2.98
		Coke	0.005	0.12	0.00	0.10–0.14
		Bituminous coal	2.620	80.37	0.69	67.50–93.32
		Lignite	0.274	10.07	0.09	8.45–11.69
		Peat	0.018	0.52	0.00	0.44–0.60
	Petroleum	Liquid petroleum gas	4.858	88.98	0.77	75.07–102.84
		Natural gas liquids	0.003	0.05	0.00	0.04–0.06
		Kerosene used	2.496	55.92	0.48	47.18–64.62
	Gas	Dry natural gas	20.048	393.32	3.38	331.83–454.64
	Biomass	Biogas	0.234	3.56	0.03	3.00–4.12
		Firewood	16.255	553.45	4.76	463.80–645.48
		Straw	17.879	375.88	3.23	316.15–435.55
		Dung cake	2.326	54.68	0.47	45.93–63.49
	Wastes	Small-scale solid waste burning	2.178	48.27	0.42	40.71–55.81
	Sub-total		72.346	1667.74	14.34	1402.36–1935.34

Table 3. Continued.

Sector	Type	Detailed sub-type	Energy, EJ yr^{-1}	CO_2, Tg C yr^{-1}	F, %	R_{90}, Tg C yr^{-1}
Transport-ation	Petroleum	Motor vehicle gasoline	41.862	755.29	6.50	637.21–872.88
		Aviation gasoline	0.057	1.02	0.01	0.86–1.18
		Jet kerosene	4.877	89.56	0.77	75.56–103.51
		Motor vehicle gas/diesel	33.334	634.98	5.46	535.73–733.87
		Oil used by ocean tanker	2.144	35.94	0.31	23.76–47.86
		Oil used by ocean container ships	1.608	26.96	0.23	17.82–35.90
		Oil used by bulk and combined carriers	1.488	25.39	0.22	16.78–33.80
		Oil used by general cargo vessels	2.600	44.36	0.38	29.33–59.07
		Oil used by non-cargo vessels	1.744	30.27	0.26	20.01–40.31
		Oil used by auxiliary engines	0.616	10.76	0.09	7.12–14.33
		Oil used by military vessels	0.355	7.93	0.07	5.25–10.56
	Biomass	Liquid biofuels used by vehicles	2.231	42.44	0.36	35.81–49.05
	Sub-total		92.916	1704.91	14.66	1405.24–2002.31
Agriculture	Petroleum	Gas/diesel used in agriculture	6.264	85.27	0.73	71.94–98.55
	Wastes	Open burning of agriculture waste	4.464	145.03	1.25	121.98–168.04
	Sub-total		10.728	230.30	1.98	193.92–266.59
Natural sources	Biomass	Biomass burned in forest fires	5.811	193.90	1.67	128.28–258.04
		Biomass burned in deforestation fires	14.570	489.52	4.21	323.86–651.43
		Biomass burned in peat fires	1.372	46.07	0.40	30.48–61.31
		Biomass burned in woodland fires	8.527	286.34	2.46	189.44–381.05
		Biomass burned in savanna fires	28.620	801.64	6.89	530.29–1066.92
	Sub-total		58.900	1817.48	15.63	1202.36–2418.75
Fuel total			533.972	11238.72	96.65	9112.29–13349.65
Cement production			0.129	388.99	3.35	328.32–449.67
Total (fuel and cement production)			534.101	11627.71	100.00	9440.61–13799.32

(Oda and Maksyutov, 2011) (Fig. 4). Differences in spatial pattern between the two inventories are large. ODIAC shows more concentrated emissions over urbanized regions with lights. Although a correlation between urban lighting and CO_2 emission has been shown on a national basis (Raupach et al., 2010; Oda et al., 2010), such a relationship is very likely to break down in populated or industrialized rural areas. For example, large CO_2 emissions from rural settlements with high population densities in Sichuan, China, identified in PKU-CO_2 do not appear strongly in satellite nightlights and ODIAC maps. Similarly, a highly emitting coking industrial zone in Qin county, China, is also associated with negligible nightlight signals (inset of Fig. 4). The underestimation of rural CO_2 emissions using nightlight spatialization has been mentioned by Oda et al. (2010). For comparison, RDs were calculated for all SDUs of the 45 sub-nationally disaggregated countries based on the PKU-CO_2 and ODIAC inventory, and E_1 (from PKU-CO_2) is considered to be the MAV. The means and standard deviations of the absolute RDs are 113 ± 67.3 % for all SDUs and range from 28.7 ± 29.2 % (8 SDUs in Australia) to 116.7 ± 67.6 % (2373 SDUs in China) for individual countries.

The second inventory to which PKU-CO_2 was compared is VULCAN (version 2.2). VULCAN (a $0.1^\circ \times 0.1^\circ$ and 1 h resolution CO_2 emission inventory for year 2002 (fossil fuel emissions only) in the USA) is perhaps one of the best emission products in terms of the amount of accurate data entering in its fabrication (Gurney et al., 2009). Over the USA, VULCAN 2.2 is closer to the true emissions than PKU-CO_2 because it uses a large number of sectoral "process-based" data that are not used in PKU-CO_2 (and not available elsewhere than in the USA). This is also the reason why we developed a top-down sub-national disaggregation approach. After normalization (at the county level to correct for the difference between 2002 and 2007), PKU-CO_2 was compared to the VULCAN 2.2 over the USA (Fig. 5). RD was calculated for each 0.1° grid point with no MAV assumed, since both inventories are based on county fuel data. Although no systematic skewness is found, more than 30 % of the grid points show a difference larger than a factor of 2 between PKU-CO_2 and VULCAN 2.2. These differences are due to the fact that detailed information used by VULCAN 2.2 is absent from PKU-CO_2, such as road GIS data and geocoded locations of point sources of industrial facilities, some commer-

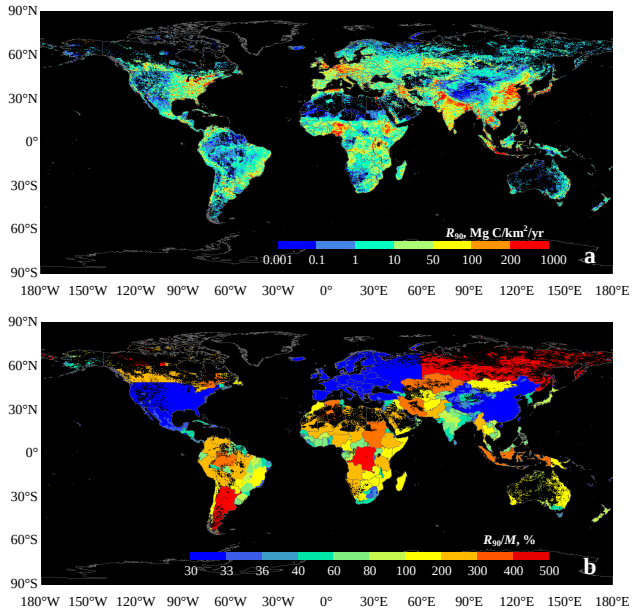

Fig. 3. Geographical distributions of absolute and relative uncertainties of CO_2 emissions from combustion sources, excluding shipping and aviation at $0.1° \times 0.1°$ resolution. **(a)** Absolute uncertainties as R_{90} and **(b)** relative uncertainties as R_{90}/M, where R_{90} and M are the 95th minus 5th percentile range and median value obtained in each grid point calculated from 1000 Monte Carlo simulations with randomly varied input data.

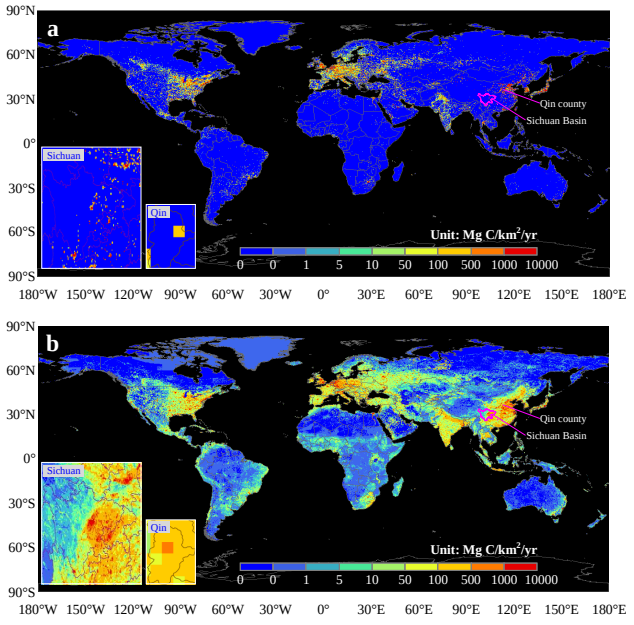

Fig. 4. Comparison between ODIAC **(a)** and PKU-CO_2 **(b)** for fossil fuel emissions excluding shipping and aviation. Emissions in a coking industrial zone in rural area of Qin county, China, and heavily populated Sichuan Basin, China, are shown in the insets at the bottom-left of the maps. The grids with zero emission are displayed in black.

cial sources, and airports. In addition, for area or nonpoint sources, CO_2 emissions were allocated from the counties to the USA Census tracts according to the area of residential/commercial/industrial building square footage and then distributed to 10 km × 10 km grids via area-based weighting in VULCAN 2.2, while they were more simply disaggregated to $0.1° \times 0.1°$ grids using the 0.8 km × 0.8 km population distribution (ORNL, 2008) in PKU-CO_2.

In addition, the improvement of the sub-national disaggregation method was also tested by comparing both PKU-CO_2 and NAT-CO_2 with VULCAN 2.2 at various spatial resolutions from 0.1° to 4° . The average absolute values of RD between PKU-CO_2 and VULCAN 2.2 were much smaller than those between the NAT-CO_2 and VULCAN 2.2 (Table S5), indicating that most of the reduction of the spatial bias of CO_2 emission maps is obtained by using fuel data at US-states scale, the rest by using realistic activity data like VULCAN 2.2 does.

4 Discussion

4.1 Differences between urban and rural areas

Uneven development of urban and rural areas is a key reason for E_{cap} variations within developing countries. It is interesting to compare E_{cap} between urban and rural areas using sub-nationally spatialized data. In Fig. 6, global fossil fuel E_{cap} of urban and rural areas are mapped separately, together with M and R_{90} for representative countries. Globally, E_{cap} were 2.41 and 0.799 Mg C/(cap. × yr) as medians for urban and rural areas, respectively. The gap between rural and urban E_{cap} was found to be very large in developing countries (2.08 vs. 0.598 Mg C/(cap. × yr)), but small in developed countries (3.55 vs. 3.41 Mg C/(cap. × yr)). For developing countries in transition (IMF, 2000), E_{cap} in urban areas is close to that of developed countries, but E_{cap} in rural areas were not much different from those of other developing countries. As a typical example, E_{cap} in China is of 3.28 and 0.691 Mg C/(cap. × yr) in urban and rural areas, respectively.

The large urban–rural E_{cap} difference in developing countries is due to uneven socioeconomic development (Satterthwaite, 2009; Dhakal, 2010). Such a difference is a key driver of future emission trends and must be addressed when formulating carbon mitigation policy. For example, China has experienced a rapid urbanization with the urban population rising from 19.6 % in 1980 to 42.2 % in 2007 (World Bank, 2010). A substantial change in economic activity and lifestyle of the new urban settlers is associated with the factor of 3.2 increase in the country E_{cap} (IEA, 2010c). It is anticipated that there will be a rapid increase of CO_2 emissions from millions of people who will continue to migrate from rural to urban areas in developing countries. Changes in the energy structure in rural areas of developing countries

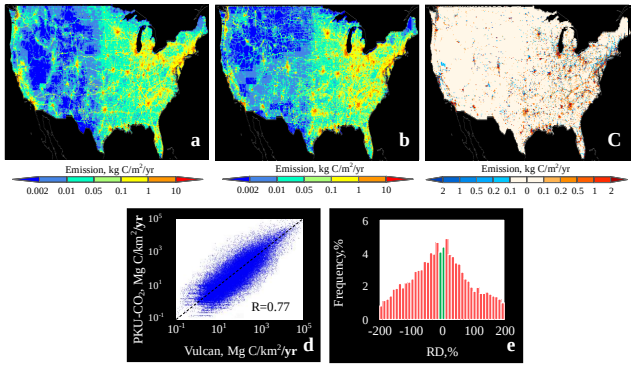

Fig. 5. Comparison between the VULCAN 2.2 (a very detailed fossil fuel CO_2 process-based emission inventory model, only available over the USA territory, normalized for individual counties to correct for the difference between 2002 and 2007) and the PKU-CO_2 inventory (this study) created at the resolution of 0.1° over the globe. **(a)** VULCAN 2.2 emissions corrected to year 2007; **(b)** the PKU-CO_2 inventory established for the year 2007; **(c)** difference plot between PKU-CO_2 and corrected VULCAN 2.2; **(d)** log-scaled scatter plot of grid-point emissions (84166 grid points) in PKU-CO_2 and corrected VULCAN 2.2; **(e)** frequency distribution of relative differences (RDs) of grid-point emissions between PKU-CO_2 and corrected VULCAN 2.2. We do not expect PKU-CO_2 to be more realistic than the VULCAN 2.2 inventory, but this comparison is shown to illustrate how PKU-CO_2 approaches VULCAN 2.2 best product over a region where the comparison is possible.

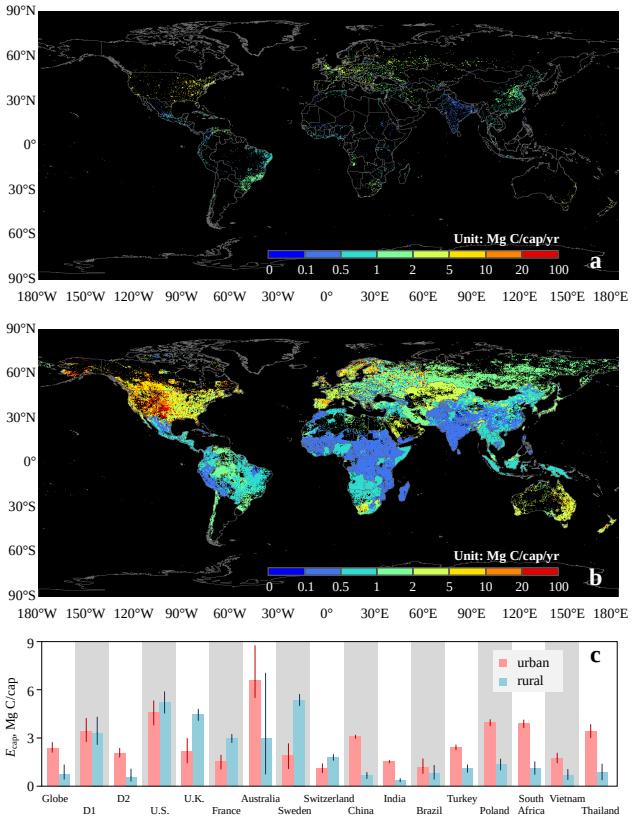

Fig. 6. Comparison in per capita fossil fuel CO_2 emissions (E_{cap}) between urban and rural areas: **(a)** urban E_{cap} map, **(b)** rural E_{cap} map, and **(c)** E_{cap} as M and R_{90} from the Monte Carlo simulations for 14 representative countries, all developed countries (D1), all developing countries (D2), and the globe. For the Monte Carlo simulations, both variations in PKU-CO_2 and urban–rural classification criteria (uniform distribution, ±10 %) are accounted for.

are also taking place with improved stoves, biogas, liquid petroleum gas, and electric appliances being used increasingly (Cai and Jiang, 2008). Although this trend could improve energy efficiency and reduce emissions of air pollutants, the replacement of traditional biomass fuels by fossil fuels and electricity may result in greater E_{cap} in rural areas as well (Solomon et al., 2007).

4.2 Impact of PKU-CO_2 emission maps on terrestrial CO_2 flux maps derived from an inversion

The spatial distribution of terrestrial CO_2 fluxes inferred using atmospheric CO_2 measurements and inverse models remains uncertain (affected with biases), partly due to the lack of emission information with high spatial and temporal resolutions (Lauvaux et al., 2009). Peylin et al. (2011) investigated the influence of using different fossil fuel emission inventories on the simulation of CO_2 in the atmosphere in Europe, and pointed out an urgent need to improve the spatially and temporally resolved CO_2 emission inventory. Therefore, reducing the uncertainty of CO_2 emission maps $F(x)$ helps to reduce uncertainty of terrestrial carbon fluxes $B(x)$ in inversions (see Sect. 2.8 for definitions). PKU-CO_2 and NAT-CO_2 were compared for deducing $B(x)$ using the CarbonTracker inversion of the net fossil + terrestrial CO_2 flux, $N(x)$ (NOAA, 2010). $B(x)$ calculated by subtracting either PKU-CO_2 or NAT-CO_2 maps from $N(x)$ are shown in Fig. 7a. With the PKU-CO_2 emission inventory, a different pattern of terrestrial CO_2 sources and sinks is obtained. To test the effect of sub-national disaggregation of emissions on $B(x)$ distribution, differences in the $B(x)$ calculated based on PKU-CO_2 and NAT-CO_2 are shown in Fig. 7b. The mean absolute difference in $B(x)$ by country is 52.2 (Mexico), 40.4 (China), 28.3 (USA), 17.9 (India), 3.05 (Brazil), and 0.681 (Australia) g C km^{-2} yr^{-1}. This simple application of PKU-CO_2 here serves only to illustrate that using a CO_2 emission map based on sub-national disaggregation method has a large indirect influence on $B(x)$. In a future study, one should prescribe PKU-CO_2 and its uncertainty to an inversion system to correct both $F(x)$ and $B(x)$ using atmospheric CO_2 observations.

5 Conclusions

PKU-FUEL and PKU-CO_2 appear to be the first global sub-nationally disaggregated 0.1° × 0.1° carbon-fuel combustion

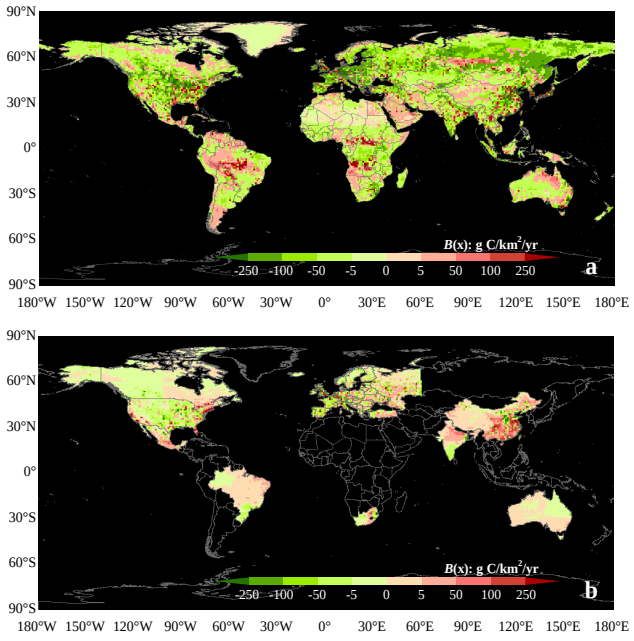

Fig. 7. Geographic distribution of terrestrial ecosystem CO_2 fluxes deduced by subtracting from the net land–atmosphere carbon flux in an atmospheric inversion CarbonTracker. **(a)** Carbon balance based on the PKU-CO_2 inventory, and the negative (positive) values correspond to carbon sinks (sources), and **(b)** map of differences in terrestrial ecosystem carbon fluxes for sub-nationally disaggregated units (SDUs) based on the PKU-CO_2 inventory and the (regionally) less accurate NAT-CO_2 inventory relying on national fuel data only for the 45 countries. The fluxes are not adjusted for other GHG exchange and crop harvest. This result also depends on the inversion model used, and the two maps are shown only as an example. The RD could not be calculated for the countries where sub-national data were not available or not reported, and these areas are displayed in black.

and CO_2 emission maps, for which an uncertainty is estimated. The major improvements of PKU-CO_2 over previous inventories are as follows: (1) a large database of sub-national fuel consumptions was used for 45 major countries, which explicitly accounts for uneven distributions of F_{cap} and E_{cap} within these countries; (2) fossil, biomass, and solid waste fuels were included and categorized into 64 types in 6 economic sectors, and (3) uncertainties of the CO_2 emission maps were quantified. The relative uncertainty range (R_{90}/M) of CO_2 emission could be reduced from 364 % to 63.2 % by using the sub-national disaggregation. In the 9 countries with sub-national data of different levels available, the spatial distortion of CO_2 emissions by using a nationally disaggregation method can be reduced by 17.5–79.8 %, indicating a substantial reduction of the spatial bias. It was also found that the degree of spatial bias reduction is larger in countries with a higher degree of imbalance or with smaller SDUs applied.

The inventory can be further improved by compiling more sub-national fuel consumption data for other large countries. Inventories with temporal resolutions, both intra- and inter-annual, are also needed. The significant difference in CO_2 emissions between urban and rural areas in transition countries suggests that more studies on the effect of rapid urbanization on CO_2 emissions should be addressed. PKU-FUEL is ready to be used for estimating emissions of other greenhouse gases, black carbon, and various air pollutants, which can help us to improve our understanding on combustion-related climate forcing and health impact. In the future, sub-national data are recommended to be reported by large countries with high differences in per capita fuel consumption, so as to reduce spatial bias in IPCC GHG reporting.

List of abbreviations

CO_2:	carbon dioxide
SDM:	sub-national disaggregation method
EF:	emission factor
F_{cap}:	per capita fuel consumption
E_{cap}:	per capita CO_2 emission
GOSAT:	Japanese Greenhouse gases Observing SATellite Project
PKU:	Peking University
PKU-FUEL:	Peking University Fuel Inventories
PKU-CO_2:	Peking University CO_2 Inventories
EUCS-36:	the 36 European countries with sub-national data
SDU:	sub-nationally disaggregated unit
Nat-CO_2:	a mock-up inventory generated based on the national fuel data and disaggregation
CO:	carbon monoxide
NO_x:	nitrogen oxide
CARMA:	Carbon Monitoring for Action
CV:	coefficient of variation
RD:	relative difference
R_{90}:	95th minus 5th percentile range
M:	median
R_{90} / M:	the ratio of R_{90} to median
ODIAC:	Open source Data Inventory of Anthropogenic CO_2 emission
IEA:	International Energy Agency
EDGAR:	The Emissions Database for Global Atmospheric Research
MAV:	more accurate value

Supplementary material related to this article is available online at: http://www.atmos-chem-phys.net/13/5189/2013/acp-13-5189-2013-supplement.zip.

Acknowledgements. Funding for this study was provided by the National Natural Science Foundation of China (41130754).

CarbonTracker 2010 results were provided by NOAA ESRL, Boulder, Colorado, USA (http://carbontracker.noaa.gov). We thank Tomohiro Oda (NOAA Earth System Research Lab, USA) and Shamil Maksyutov (National Institute for Environmental Studies, Japan) for providing the original data of ODIAC and valuable comments, Christopher D. Elvidge (NOAA National Geophysical Data Center, USA) for helping us to retrieve natural gas flaring data, and Brian Reid (University of East Anglia, UK) and Matthew J. McGrath (Laboratoire des Sciences du Climat et de l'Environnement, France) for valuable comments and proof-reading.

Edited by: P. Monks

References

Andreae, M. O. and Merlet, P.: Emission of trace gases and aerosols from biomass burning, Global Biogeochem. Cy., 15, 955–966, 2001.

Andres, R. J., Marland, G., Fung, I. E., and Matthews, E. A.: $1^\circ \times 1^\circ$ distribution of carbon dioxide emissions from fossil fuel consumption and cement manufacture, 1950-1990, Global Biogeochem. Cy., 10, 419–429, 1996.

American Petroleum Institute (API): Compendium of Greenhouse Gas Emissions Estimation Methodologies for the Oil and Gas Industry, Pilot Test Version, available at: http://www.api.org/environment-health-and-safety/climate-change/whats-new/compendium-ghg-methodologies-oil-and-gas-industry, 2001.

Australian Bureau of Agricultural and Resource Economics and Sciences (ABES): Energy in Australia 2008, available at: http://www.abares.gov.au/publications, 2008.

Bocquet, M.: Grid resolution dependence in the reconstruction of an atmospheric tracer source, Nonlinear Proc. Geophy., 34, 521–529, 2005.

Bond, T. C., Streets, D. G., Fernandes, S. D., Nelson, S. M., Yarber, K. F., Woo, J.-H., and Klimont, Z.: A technology-based global inventory of black and organic carbon emissions from combustion, J. Geophys. Res. Atmos., 109, D14203, doi:10.1029/2003JD003697, 2004.

Brazil Energy Ministry: Brazil Energy Statistics, available at: http://www.mme.gov.br/mme, 2010.

British Petroleum (BP): Statistical Review of World Energy-2007, available at: http://www.bp.com, 2008.

Cai, J. and Jiang, Z.: Changing of energy consumption patterns from rural households to urban households in China: an example from Shaanxi Province, China, Renew. Sust. Energ. Rev., 12, 1667–1680, 2008.

Cao, G. L., Zhang, X. Y., Wang, D., and Zheng, F. C.: Inventory of emissions of pollutants from open burning crop biomass, J. Agr. Environ. Sci. 24, 800–804, 2005.

Centre on Emission Inventories and Projections (CEIP): Emissions as used in EMEP models, available at: http://www.ceip.at (last access: 14 August 2012), 2011.

Ciais, P., Paris, J. D., Marland, G., Peylin, P., Piao, S. L., Levin, I., Pregger, T., Scholz, Y., Friedrich, R., Rivier, L., Houwelling, S., Schulze, E. D., and members of the CARBOEUROPE SYNTHESIS TEAM (1): The European carbon balance, Part 1: fossil fuel emissions, Global Change Biol., 16, 1395–1408, 2010.

Davis, S. J., Caldeira, K., and Matthews, H. D.: Future CO_2 emissions and climate change from existing energy infrastructure, Science, 329, 1330–1332, 2010.

Dhakal, S.: GHG emissions from urbanization and opportunities for urban carbon mitigation, Curr. Opin. Env. Sust., 2, 277–283, 2010.

Elvidge, C. D., Ziskin, D., Baugh, K. E., Tuttle, B. T., Ghosh, T., Pack, D. W., Erwin, E. H., and Zhizhin, M.: A fifteen year record of global natural gas flaring derived from satellite data, Energies, 2, 595–622, 2009.

Environment Canada/Natural Resource Canada: State Energy Statistics 2007, available at: www.nrcan.gc.ca, 2010.

Equasis: The world merchant fleet in 2007 (Lisbon), available at: http://www.equasis.org/EquasisWeb/public/HomePage (last access: 14 August 2012), 2008.

European Commission: Joint Research Centre (JRC)/Netherlands Environmental Assessment Agency (PBL). Emission Database for Global Atmospheric Research (EDGAR), release version 4.2. http://edgar.jrc.ec.europa.eu, 2011.

Eyers, V., Kohler, H. W., van Aardenne, J., and Lauer, A.: Emissions from international shipping: 1. The last 50 years, J. Geophys. Res., 110, D17305, doi:10.1029/2004JD005619, 2005.

Food and Agriculture Organization of the United Nations (FAO): FAOSTAT food and agriculture statistics, available at: http://faostat.fao.org/default.aspx, 2010.

Friedl, M. A., Mclver, D. K., Hodges, J., Zhang, X. Y., Muchoney, D., Strahler, A. H., Woodcock, C. E., Gopal, S., Schneider, A., Cooper, A., Baccini, A., Gao, F., and Schaaf, C.: Global land cover mapping from MODIS: algorithms and early results, Remote Sens. Environ., 83, 287–302, 2002.

Gurney, K. R., Mendoza, D. L., Zhou, Y., Fischer, M. L., Miller, C. C., Geethakumar, S., and de la Rue du Can, S.: High resolution fossil fuel combustion CO_2 emission fluxes for the United States, Environ. Sci. Technol., 43, 5535–5541, 2009.

Intergovernmental Panel on Climate Change (IPCC): Revised 1996 IPCC Guidelines for National Greenhouse Gas Inventories, Reference Manual (Volume 3), United Nations Environment Programme, the Organization for Economic Co-operation and Development, the International Energy Agency, IPCC, available at: http://www.ipcc-nggip.iges.or.jp/public/gl/invs1.htm, 1996.

International Energy Agency (IEA): Energy Statistics and Balances of OECD Countries, 2007–2008, Paris, 2010a.

International Energy Agency (IEA): Energy Statistics and Balances of Non-OECD Countries, 2007–2008, Paris, 2010b.

International Energy Agency (IEA): CO_2 Emission From Fuel Combustion-2011 Highlights, Paris, 2010c.

International Monetary Fund (IMF): Transition Economies: An IMF Perspective on Progress and Prospects, available at: http://www.imf.org/external/np/exr/ib/2000/110300.htm, 2000.

Johnson, M., Edwards, R., Frenk, C. A., and Masera, O.: In-field greenhouse gas emissions from cookstoves in rural Mexican households, Atmos. Environ., 42, 1206–1222, 2008.

Lauvaux, T., Pannekoucke, O., Sarrat, C., Chevallier, F., Ciais, P., Noilhan, J., and Rayner, P. J.: Structure of the transport uncertainty in mesoscale inversions of CO_2 sources and sinks using ensemble model simulations, Biogeosciences, 6, 1089–1102, doi:10.5194/bg-6-1089-2009, 2009.

Lee, S., Baumann, K., Schauer, J. J., Sheesley, R. J., Naeher, L. P., Meinardi, S., Blake, D. R., Edgerton, E. S., Russell, A. G., and Clements, M.: Gaseous and particulate emissions from prescribed burning in Georgia, Environ. Sci. Technol., 39, 9049–

9056, 2005.

Marland, G.: Uncertainties in Accounting for CO_2 From Fossil Fuels, J. of Indust. Ecol., 12, 136–139, doi:10.1111/j.1530-9290.2008.00014.x, 2008.

Marland, G., Rotty, R. M., and Treat, N. L.: CO_2 from fossil fuel burning: global distribution of emissions, Tellus B, 37, 243–258, 1985.

Ministry of Agriculture of China (MAC): China Agriculture Yearbook 2008, China Agriculture Press, Beijing, 2008.

National Bureau of Statistics (NBS): China Energy Statistical Yearbook 2007, China Statistics Press, Beijing, 2008.

NOAA Earth Observation Group: Global Gas Flaring Estimates, available at: http://www.ngdc.noaa.gov/dmsp/interest/gasflares.html, 2011.

NOAA Earth System Research Laboratory/Global Monitoring Division: CarbonTracker $1^\circ \times 1^\circ$ Land Fluxes Datasets, available at: http://carbontracker.noaa.gov, 2010.

Nyboer, J., Strickland, C., and Tu, J. J.: Improved CO_2 , CH_4 and N_2O Emission Factors for Producer-Consumed Fuels in Oil Refinerie, Canadian Industrial End-use Energy Data and Analysis Centre, 2006.

Oak Ridge National Laboratory (ORNL): LandScan Global Population 2007 Database, available at: http://www.ornl.gov/sci/landscan/, 2008.

Oda, T. and Maksyutov, S.: A very high-resolution ($1\,km \times 1\,km$) global fossil fuel CO_2 emission inventory derived using a point source database and satellite observations of nighttime lights, Atmos. Chem. Phys., 11, 543–556, doi:10.5194/acp-11-543-2011, 2011.

Oda, T., Maksyutov, S., and Elvidge, C. D.: Disaggregation of national fossil fuel CO_2 emissions using a global power plant database and DMSP nightlight data, Proc. of the 30th Asia-Pacific Advanced Network Meeting, 220–229, 2010.

Penner, J. E., Eddleman, H., and Novakov, T.: Towards the development of a global inventory for black carbon emissions, Atmos. Environ., Part A, 27, 1277–1295, 1993

Peters, W., Jacobson, A. R., Sweeney, C., Andrews, A. E., Conway, T. J., Masarie, K., Miller, J. B., Bruhwiler, L. M. P., Petron, G., Hirsch, A. I., Worthy, D. E. J., van der Werf, G. R., Randerson, J. T., Wennberg, P. O., Krol, M. C., and Tans, P. P.: An atmospheric perspective on North American carbon dioxide exchange: CarbonTracker, P. Natl. Acad. Sci. USA, 104, 18925–18930, 2007.

Peylin, P., Houweling, S., Krol, M. C., Karstens, U., Rödenbeck, C., Geels, C., Vermeulen, A., Badawy, B., Aulagnier, C., Pregger, T., Delage, F., Pieterse, G., Ciais, P., and Heimann, M.: Importance of fossil fuel emission uncertainties over Europe for CO_2 modeling: model intercomparison, Atmos. Chem. Phys., 11, 6607–6622, doi:10.5194/acp-11-6607-2011, 2011.

Pillai, D., Gerbig, C., Marshall, J., Ahmadov, R., Kretschmer, R., Koch, T., and Karstens, U.: High resolution modeling of CO_2 over Europe: implications for representation errors of satellite retrievals, Atmos. Chem. Phys., 10, 83–94, doi:10.5194/acp-10-83-2010, 2010.

Raupach, M. R., Rayner, P. J., and Paget, M.: Regional variations in spatial structure of night-lights, population density and fossil-fuel CO_2 emissions, Energ. Policy. 38, 756–4764, 2010.

Rayner, P. J., Raupach, M. R., Paget, M., Peylin, P., and Koffi, E.: A new global gridded dataset of CO_2 emissions from fossil fuel combustion: Methodology and evaluation, J. Geophys. Res., 115, D19306, doi:10.1029/2009JD013439, 2010.

Satterthwaite, D.: The implications of population growth and urbanization for climate change, Environ. Urban., 21, 545–567, 2009.

Solomon, S., Qin, D., Manning, M., Chen, Z., Marquis, M., Averyt, K. B., Tignor, M., and Miller, H. L.: IPCC Climate Change 2007: The Physical Science Basis, Cambridge University Press, Cambridge, 2007.

Statistics South Africa: Energy Accounts for South Africa: 2002–2006, Statistics South Africa, Pretoria, 2009.

Streets, D., Yarber, K., Woo, J. H., and Carmichael, G. R.: Biomass burning in Asia: annual and seasonal estimates and atmospheric emissions, Global Biogeochem. Cy., 17, 1099, doi:10.1029/2003GB002040, 2003.

Tata Energy Research Institute (TERI): Tata Energy Directory and Data Yearbook 2007, New Delhi, India, 2008.

Tie, X., Brasseur, G., and Ying, Z.: Impact of model resolution on chemical ozone formation in Mexico City: application of the WRF-Chem model, Atmos. Chem. Phys., 10, 8983–8995, doi:10.5194/acp-10-8983-2010, 2010.

Turkish Statistical Institute (TSI): Turkish Statistical Institute Regional Statistics 2007, available at: http://tuikapp.tuik.gov.tr/Bolgesel/sorguSayfa.do?target=tablo, 2010.

Ummel, K.: CARMA revisited: an updated database of carbon dioxide emissions from power plants worldwide, Center for Global Development, Working Paper 304, 2012.

UN Industrial Development Organization (UNID): International Yearbook of Industrial Statistics 2008, Edward Elgar Publishing, Inc. Cheltenham, Glos GL50 1UA, UK, 2008.

United Nations Statistics Division (UNSD): Environmental Indicators: Waste, available at: http://unstats.un.org/unsd/environment/qindicators.htm, 2010.

US Department of Energy: Instructions for Form EIA 1605 Voluntary Reporting of Greenhouse Gases, Appendix B – Fuel and Energy Source Codes and Emission Coefficients, available at: http://www.eia.gov/oiaf/1605/reportingformprelaunch.html (last access: 14 August 2012), 2000.

United States Energy Information Administration (USEIA): State Energy Data, available at: http://www.eia.gov/state/, 2008.

United States Energy Information Administration (USEIA): World Carbon Dioxide Emissions from the Use of Fossil Fuels (Washington DC), available at: http://www.eia.gov/cfapps/ipdbproject/IEDIndex3.cfm?tid=90&pid=44&aid=8, 2010.

United States Environmental Protection Agency (USEPA): Mexico national emissions inventory, available at: http://www.epa.gov/ttn/chief/net/mexico.html, 2006.

United States Environmental Protection Agency (USEPA): Emission factor documentation for AP-42, available at: http://www.epa.gov/ttn/chief/ap42/index.html, 2008.

United States Environmental Protection Agency (USEPA): National Emissions Inventory Data & Documentation (USEPA, Research Triangle Park, NC), available at: http://www.epa.gov/ttn/chief/net/2008inventory.html, 2011.

United States Geological Survey (USGS): Aluminum Statistics and Information 2007, available at: http://minerals.usgs.gov/minerals/pubs/commodity/aluminum/, 2010a.

United States Geological Survey (USGS): Cement Statistics and Information 2007, available at: http://minerals.usgs.gov/minerals/pubs/commodity/cement/, 2010b.

URS: Corporation EME Greenhouse Gas Emission Factor Review – Final Technical Memorandum, Austin, Texas, 2003.

van der Werf, G. R., Randerson, J. T., Giglio, L., Collatz, G. J., Mu, M., Kasibhatla, P. S., Morton, D. C., DeFries, R. S., Jin, Y., and van Leeuwen, T. T.: Global fire emissions and the contribution of deforestation, savanna, forest, agricultural, and peat fires (1997–2009), Atmos. Chem. Phys., 10, 11707–11735, doi:10.5194/acp-10-11707-2010, 2010.

Wang, C., Corbett, J. J., and Firestone, J.: Improving spatial representation of global ship emissions inventories, Environ. Sci. Technol., 42, 193–199, 2008.

Wheeler, D. and Ummel, K.: Calculating CARMA: global estimation of CO_2 emissions from the power sector. Center for Global Development, Working Paper 145, 2008.

World Bank: World Development Indicators, available at: http://databank.worldbank.org/ddp/home.do, 2010.

Yevich, R. and Logan, J. A.: An assessment of biofuel use and burning of agricultural waste in the developing world, Global Biogeochem. Cy., 17, 2002GB001952, 2003.

Yokota, T., Yoshida, Y., Eguchi, N., Ota, Y., Tanaka, T., Watanabe, H., and Maksyutov, S.: Global concentrations of CO_2 and CH_4 retrieved from GOSAT: first preliminary results, SOLA, 5, 160–163, 2009.

Zhang, H., Ye, X., Cheng, T., Chen, J., Yang, X., Wang, L., and Zhang, R.: A laboratory study of agricultural crop residue combustion in China: emission factors and emission inventory, Atmos. Environ., 42, 8432–8441, 2008.

Zhang, Y. X. and Tao, S.: Global atmospheric emission inventory of polycyclic aromatic hydrocarbons (PAHs) for 2004, Atmos. Environ., 43, 812–819, 2009.

Zhang, Y. X., Tao, S., Cao, J., and Coveney, R. M.: Emission of polycyclic aromatic hydrocarbons in China by county. Environ. Sci. Technol., 41, 683–687, 2007.